Kinetics of Ca^{2+} Binding to the SR Ca-ATPase in the E_1 State

Christine Peinelt and Hans-Jürgen Apell
Department of Biology, University of Konstanz, Konstanz, Germany

ABSTRACT The time-resolved kinetics of Ca^{2+} binding to the SR Ca-ATPase in the E_1 state was investigated by Ca^{2+}-concentration jump experiments. Ca^{2+} was released by an ultraviolet-light flash from caged calcium, and charge movements in the membrane domain of the ion pumps were detected by the fluorescent styryl dye 2BITC. The partial reaction ($H_3E_1 \leftrightarrow$) $E_1 \leftrightarrow CaE_1 \leftrightarrow Ca_2E_1$ can be characterized by two time constants, τ_1 and τ_2, both of which are not significantly Ca^{2+}-concentration-dependent and only weakly pH-dependent at pH < 7.5. Both time constants differ by a factor of $\sim$50 (4.7 vs. 200 ms). The weak substrate-dependence indicates that the rate-limiting process is not related to Ca^{2+} migration through the access channel and ion binding to the binding sites but to conformational rearrangements preceding the ion movements. The high activation energy obtained for both processes, 42.3 kJ mol^{-1} and 60.3 kJ mol^{-1} at pH 7.2, support this concept. Transient binding of Ca ions to the loop L67 and a movement of the Ca-loaded loop are discussed as a mechanism that facilitates the entrance of both Ca ions into the access channel to the ion-binding sites.

INTRODUCTION

The physiological task of the Ca-ATPase of the sarcoplasmic reticulum (SR) is to restore the Ca ions released upon excitation in their internal storage and to enable muscle relaxation within 50 ms after a contraction (1). Performing this task the enzyme undergoes different states while running through its pump cycle. This cycle, the so-called Post-Albers cycle, describes transport of two Ca^{2+} from the cytosol to the SR lumen and, subsequently, counters transport of two H^+ in a Ping-Pong mode while the enzyme is phosphorylated in the first and dephosphorylated in the second half cycle. The enzymatic partial reactions catalyze the transition between both basic conformations, E_1, in which the ion-binding sites are accessible from the cytoplasm, and P-E_2, in which the binding sites are opened to the luminal aqueous phase. It is shown that the ion-binding and release steps in both conformations are electrogenic, i.e., net electric charges are moved into and out of the membrane dielectric (2,3). These findings can be explained by the concept that the ion-binding sites are located (almost) in the middle of the membrane domain of the SR Ca-ATPase (4). Recently published structures of the SR Ca-ATPase in four different states, Ca_2E_1, ATP·E_1 (stabilized by E_1·AMPPCP), P$\sim E_2$, (obtained as $E_2 \cdot MgF_4^{2-}$), and E_2·Thapsigargin confirm this claim (5–10). Although these structures present snapshots of defined enzyme conformations, kinetical investigations provide information about conformational rearrangements that the pumps have to go through when they convert from one state to another.

Since binding (or release) of ions to (or from) the SR Ca-ATPase is electrogenic, these reaction steps can be detected by the styryl dye 2BITC (11). Binding and release of H^+ and Ca^{2+} in both states have been analyzed by equilibrium titration experiments, and the respective dissociation constants were obtained (2).

To determine the rate constants that control the transition between different enzyme states, caged compounds were used to produce concentration jumps of pump substrates to trigger transitions into new equilibrium states. After a flash-induced release of ATP from its inactive precursor, caged ATP, in the presence of cytoplasmic Ca^{2+}, the Ca-ATPase undergoes enzyme phosphorylation, $Ca_2E_1 \rightarrow (Ca_2)E_1$-P, conformation transition, $(Ca_2)E_1$-P $\rightarrow$ P-E_2Ca_2, Ca^{2+} release, P-$E_2Ca_2 \rightarrow$ P-E_2, and binding of protons, P-$E_2 \rightarrow$ P-E_2H_2. Such experiments were used to determine the rate-limiting steps of the partial reactions, the conformation transition, and luminal H^+ binding (3). Another substrate of the Ca-ATPase is the transported ion, Ca^{2+}. In 1988, the application of a caged Ca was introduced to characterize Ca^{2+} binding to the enzyme (12,13). The cage, DM-Nitrophen, is a photolabile chelator of Ca^{2+} that is split by an intense ultraviolet (UV) light flash. This compound is commercially available, and allows a release of Ca^{2+} within less than a microsecond.

Since the reaction $HE_1 \rightarrow Ca_2E_2$ is electrogenic, it can be detected by the fluorescent electrochromic styryl dye 2BITC (2), and due to a response time of the dye far below a microsecond, charge movements as fast as the Ca^{2+} release from its caged chelator can be detected. This reaction sequence includes not only the release of protons from the pump and Ca^{2+} binding to the pump but also conformational rearrangements of the protein, which were detected previously by spectroscopic methods (14,15). Experiments with radioactive Ca^{2+} have shown that the two Ca^{2+} are bound to the

Submitted June 9, 2005, and accepted for publication July 13, 2005.

Address reprint requests to Hans-Jürgen Apell, Dept. of Biology, University of Konstanz, Fach M635, 78457 Konstanz, Germany. Tel.: 49-7531-88-2253; Fax: 49-7531-3183; E-mail: h-j.apell@uni-konstanz.de.

Christine Peinelt's present address is Queen's Medical Center, UHT 8, 1301 Punchbowl St., Honolulu, HI 96813.

0006-3495/05/10/2427/07 $2.00

doi: 10.1529/biophysj.105.068411

E_1 conformation in an ordered and sequential fashion (16–19). Binding of Ca^{2+} is cooperative (17), binding of the first Ca^{2+} induces (formation and) access to a binding site for the second Ca^{2+} (20). After binding of the second Ca^{2+} enzyme activation occurs (21). The presence of two defined Ca^{2+} binding sites, I and II, led to the model of Ca^{2+} single-file binding (22). The entry path of Ca^{2+} from the cytosol to the binding sites I and II is yet not fully identified, although there is evidence that it is lined up with polar residues (23). There is no water-filled vestibule visible as it is observed in ion channels (24).

According to a recent review, Glu^{309} may play a role in gating the ions to the binding sites (23). This model was also proposed from mutagenesis studies (25). After the first Ca^{2+} has bound, the second Ca^{2+} is binding to site II with a higher affinity, since the region of Asp^{800} looses flexibility after binding of the first Ca^{2+} (26).

In this study, we present time-resolved experiments of Ca^{2+} binding to the SR Ca-ATPase. The dependence of the rate constants on Ca^{2+} concentration, pH, and temperature support the concept of a conformational relaxation between binding of the first and second Ca^{2+}, and allowed us to introduce constraints for possible mechanisms of structure-function models.

MATERIALS AND METHODS

Materials

Phosphoenolpyruvate, pyruvate kinase, lactate dehydrogenase, NADH, and the Ca^{2+} carrier A23187 were obtained from Boehringer (Mannheim, Germany). DMNP-EDTA, caged Calcium (1-(4,5-dimethoxy-2-nitrophenyl)-1,2-diaminoethane-*N*,*N*,*N*′,*N*′-tetraacetic acid, and the chelator BAPTA (1,2bis(2-aminophenoxy)-ethane-*N*,*N*,*N*9,-tetrasodium salt, B1214), were obtained from MoBiTec (Göttingen, Germany). Thapsigargin was purchased from Sigma (Munich, Germany). DM-Nitrophen tetrasodium salt (caged calcium) was purchased from Calbiochem (EMD Biosciences, San Diego, CA). The styryl dye 2BITC (27) was a gift from Dr. H.-D. Martin, University of Düsseldorf, Düsseldorf, Germany. All other reagents were the highest grade commercially available.

Enzyme preparations and reconstitution

Ca-ATPase was prepared by a slight modification of the method of Heilmann et al. (28) from the *psoas* muscles of rabbits. The whole procedure was performed at temperatures below 4°C. The determination of the protein content of the membrane preparation was performed according to Markwell. The most active fractions of the final density gradient separation had a protein content of 2–3 mg ml^{-1}. The enzyme activity was determined by the linked pyruvate kinase/lactate dehydrogenase assay. Background enzyme activity of the isolated preparation was measured by addition of 1 μM thapsigargin that blocks the SR Ca-ATPase completely. The Ca-ATPase-specific activity was 175 μmol P_i per mg protein and h at 37°C and could be increased up to 310 μmol P_i per mg protein and h in the presence of A23187 to short-circuit the vesicles forming membranes for Ca^{2+}. With a molecular weight of 110,000 g mol^{-1} and a specific activity of 5.2 units mg^{-1}, the turnover rate of the pump is 9.5 s^{-1} in this preparation. In control experiments, the effect of the styryl dye 2BITC on the enzymatic activity was checked. Up to a dye concentration of 1.2 mM, no changes of the enzymatic activity could be observed.

Detection of partial reactions with 2BITC

The fluorescence measurements in equilibrium-titration experiments were performed with a self-constructed setup using a HeNe laser with a wavelength of 543 nm (Laser 2000, Wessling, Germany) to excite the fluorescence of the electrochromic dye 2BITC (2). The emitted light was collected perpendicularly to the incident light, filtered by a narrow-band interference filter (λ_{max} = 589 nm, half-width 10.6 nm) and detected by a head-on photo multiplier (R2066, Hamamatsu Photonics, Hamamatsu City, Japan). The photo current was amplified by a Keithley current amplifier 427 (Keithley Instruments, Cleveland, OH) and collected by a data-acquisition board of a PC (PCI-T112, Imtec, Backnang, Germany) with sampling frequencies between 1 and 10 Hz. The experimental data were displayed on the monitor, stored and analyzed on the PC. The temperature in the cuvette (2 ml) was maintained by a thermostat at 20°C.

For data recording of fluorescence signals with high time-resolution a setup was used, whose design was published earlier (3). A cylindrical quartz cuvette (internal diameter, 7.8 mm) containing 300 μl buffer (layer height, ~5 mm) was placed in the upper focus of an ellipsoidal mirror (Melles-Griot, Zevenaar, Netherlands) whose opening was directed downwards. The buffer contained 600 nM 2BITC, 18 μg Ca-ATPase preparation, 50 μM DM-Nitrophen and the pH was adjusted by HCl to certain values. The residual concentration of Ca^{2+} was estimated to 14 μM. The dye was excited by a 543-nm HeNe laser from the top of the setup. A quartz lens was adjusted to widen the laser beam and to illuminate the whole solution almost homogeneously. The emitted light was collected by the ellipsoidal mirror and reflected into the second focus of the mirror. An interference light filter (589 ± 10 nm) selected the emitted light of the styryl dye before passing the entrance window of a photo multiplier (R928, Hamamatsu Photonics). The output current was amplified by an I/V converter and fed into a 12-bit data-acquisition board of a PC with sampling frequencies between 1 and 500 kHz. The bottom of the cuvette was in contact with a thermostated copper socket (that also stopped the incident light). To release Ca^{2+} from its precursor, caged Ca, an UV-light flash (wavelength 350 nm, maximum power 6 MW) was generated by an EMG 100 excimer laser (Lambda Physics, Göttingen, Germany) and directed through a quartz lens into the cuvette, illuminating the whole buffer volume. The amount of released Ca^{2+} was dependent on the intensity of the UV flash and buffer pH. Approximately 30 nM at high pH and 100 nM at low pH could be obtained by the first flash. By successive light flashes, the Ca^{2+} concentration could be increased stepwise. Typically, four flashes had to be applied to saturate the binding sites of the SR Ca-ATPase with Ca^{2+}. Further flash-induced Ca^{2+} release induced no further fluorescence changes. To calibrate the respective Ca^{2+} concentrations after a flash-induced concentration jump, equilibrium titration experiments were performed in corresponding buffers at various pH, and the relative fluorescence changes and the known Ca^{2+} concentrations could be correlated with high precision (2).

To optimize the signal/noise ratio, seven measurements under identical conditions were averaged. The time course of the fluorescence signal was analyzed by a numerical fit of the data with a sum of two exponential functions,

$$F(t) = F_1 \times e^{(-t/\tau_1)} + F_2 \times e^{(-t/\tau_2)} + F_\infty, \qquad (1)$$

which provided two time constants, τ_1 and τ_2, as well as the respective fluorescence amplitudes, F_1 and F_2, and the new stationary fluorescence level, F_∞, after the relaxation process, which was used to determine the Ca^{2+} concentration.

RESULTS

To study the Ca^{2+} binding to the SR Ca-ATPase binding sites from the cytoplasmic aqueous phase in the E_1 conformation, 18 μg of Ca-ATPase, in form of isolated SR vesicles, was incubated in buffer containing 50 mM

HEPES, 600 nM 2BITC, 50 μM DM-Nitrophen, and a pH in the range between 6.3 and 8.2. At high pH the nominal free concentration was ~3 nM Ca^{2+}. The Ca^{2+} concentration was increased in a fast, steplike manner by a UV flash to ~30 nM, as could be determined from the fluorescence decrease. Subsequent flashes led to further decreases of the fluorescence amplitude until, at a concentration of ~200 nM (at pH 8.2), a saturation of the binding sites was reached (Fig. 1 *A*).

The fluorescence decrease, which reflects binding of Ca^{2+} to the enzyme in its E_1 conformation, could not be fitted satisfactorily with a single exponential function but with the sum of two exponential functions. A typical example of response to the first flash at pH 7.2 is shown in Fig. 1 *B*. This observation indicates that at least two different processes take place when the ion pumps respond on the stepwise elevation of the Ca^{2+} concentration. These (rate-limiting) reaction steps were characterized by the time constants τ_1 of the faster and τ_2 of the slower process. The corresponding fluorescence amplitudes account for the electrogenic Ca^{2+} binding to the binding sites of the enzyme. These fluorescence amplitudes do not necessarily represent the rate-limiting step if the electrogenic ion movements inside the membrane domain are separate and fast (i.e., diffusion-controlled) processes. The time constant of the fast process, τ_1, ranged from 2 to 8 ms and that of the slow process, τ_2, from 50 to 200 ms.

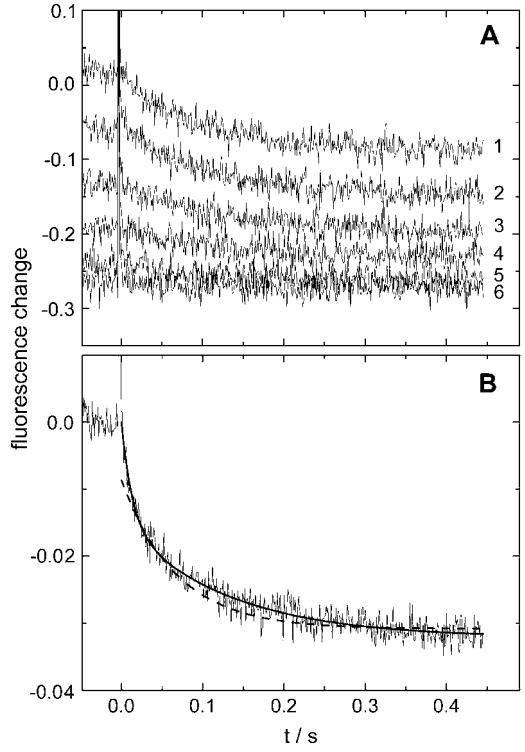

FIGURE 1 Ca^{2+}-concentration jump induced partial reactions of the SR Ca-ATPase in its E_1 conformation detected by the electrochromic styryl dye 2BITC. (*A*) After a UV flash induced Ca^{2+} release, binding of Ca^{2+} to the SR Ca-ATPase induces a decrease in 2BITC fluorescence. The initial fluorescence level of the next flash represents the enzyme's steady-state level of the previous flash. After approximately four flashes, no further fluorescence decrease could be detected, since the Ca^{2+} binding sites in the E_1 conformation are saturated with Ca^{2+}. (*B*) To obtain a significantly reduced signal/noise ratio, seven measurements under identical conditions (pH 7.2, $T = 20°C$) were averaged. The fluorescence decay could be fitted perfectly by the sum of two exponentials (Eq. 1), with the time constants $\tau_1 = 6.3$ ms and $\tau_2 = 131$ ms (*solid line*). Fitting the time course with a single exponential (*dotted line*) led to a poor agreement with the data.

A successful approach to identify the molecular processes controlling the time course of the fluorescence changes is the investigation of their dependence on the Ca^{2+} concentration and pH. Ca^{2+} and H^+ are able to enter the ion-binding sites, and may interact additionally with other moieties of the protein surface, thus producing allosteric effects, especially in the case of protons. Therefore, detailed studies on the dependency of the kinetics on both substrates, Ca^{2+} and H^+, and on the temperature, were performed.

Ca^{2+} concentration dependence

Since the observed fluorescence changes upon Ca^{2+} release were always decreasing signals, it was clear that, according to the detection mechanism of the styryl dye 2BITC, a (net) uptake of positive charges, i.e., Ca^{2+}, into the membrane domain of the pumps were observed (11). Therefore, it could be expected that the kinetics of this process would be affected by the free Ca^{2+} concentration. The concentration range in which experiments could be analyzed was between 18 nM and 2 μM. Fig. 2 *A* shows the result of the analysis of the time-dependent fluorescence decrease after the flash-induced Ca^{2+}-concentration jump. As illustrated in Fig. 1 *B*, the time course could be fitted and characterized by two time constants, τ_1 and τ_2. In the range above 50 nM, both processes were not significantly dependent on the Ca^{2+} concentration. The fast process could be described by an average time constant, τ_1, of 4.7 $\pm$ 0.5 ms (without the data points <50 nM). This corresponds to a rate constant of 213 s^{-1}. The slow process had an average time constant, τ_2, of 0.20 $\pm$ 0.01 s, or a respective rate constant of 5 s^{-1}. The deviating smaller time constants at low Ca^{2+} concentrations (<50 nM) could be obtained only in buffer with high pH, due to the pH-dependent binding affinity of caged Ca. Therefore, the lowest data points do not show a real Ca^{2+} dependence but a pH effect (see below). The ratio of both time constants was approximately a factor of 50, and both processes controlling the rate-limiting steps are obviously not reactions that are dependent on the free Ca^{2+} concentration in the buffer.

The amplitude of the fluorescence decrease of both processes F_1 and F_2 (Eq. 1), was rather small ($-1\% > F_1 + F_2 > -5\%$, data not shown). Therefore, the Ca^{2+}-concentration dependences of both amplitudes could not be determined as accurately as the time constants. When the data points of F_1 were fitted with a binding isotherm, a half-saturating concentration of 30 $\pm$ 12 nM was obtained (Fig. 2

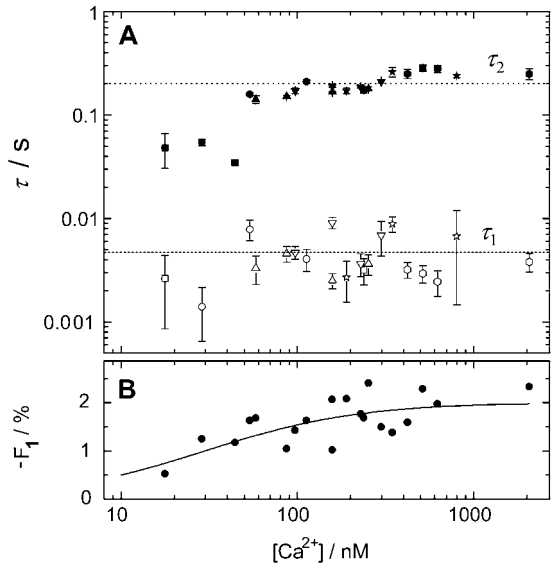

FIGURE 2 Ca^{2+}-concentration dependence of the Ca^{2+}-induced partial reactions. (*A*) The time constants τ_1 (*open symbols*) and τ_2 (*solid symbols*) were obtained from the fluorescence decrease (see Fig. 1) of experiments at various measurements of pH to vary the pH-dependent release of Ca^{2+} from caged Ca (pH 6.28, *hexagons*; pH 6.6, *stars*; pH 6.91, *down-triangles*; pH 7.1, *up-triangles*; pH 7.5, *squares*; and pH 8.2, *circles*). The respective Ca^{2+} concentrations were determined from the steady-state fluorescence after the UV flash. The lines represent the average time constants of the data points, $\tau_1 = 4.7 \pm 0.5$ ms and $\tau_2 = 200 \pm 10$ ms. (*B*) The fluorescence amplitude, F_1, of the faster process was obtained from the fit to the data. The line represents a binding isotherm with a half-saturating concentration of 30 ± 12 nM.

B) in agreement with results from equilibrium titration experiments (2). The maximum value of F_1 was $-2\% \pm 0.3\%$. The amplitude F_2 was not significantly dependent on the Ca^{2+} concentration and had a value of $-2.7\% \pm 0.3\%$.

pH dependence

Corresponding to the experiments shown in Fig. 1, measurements were performed in buffers at various pH values in the range between 6.3 and 8.2. In the whole pH range, the fluorescence decrease showed a time course that had to be fitted by two exponentials. Both the fast and the slow processes were, in a similar manner, dependent on pH, as shown in Fig. 3. Independent of the pH, the ratio between both time constants was again ~50. The lines in Fig. 3 are drawn to guide the eye; they have the same shape, and are shifted only by a factor of 50. The larger error bars of τ_1 were caused by the smaller amplitude of the fast process (~20% of the total amplitude). At higher proton concentrations in the buffer, both processes were slowed down.

Temperature dependence

Both time constants of the Ca^{2+}-induced fluorescence drop, τ_1 and τ_2, were determined in a temperature range from 7°C to 36°C. The experiments were performed with initially

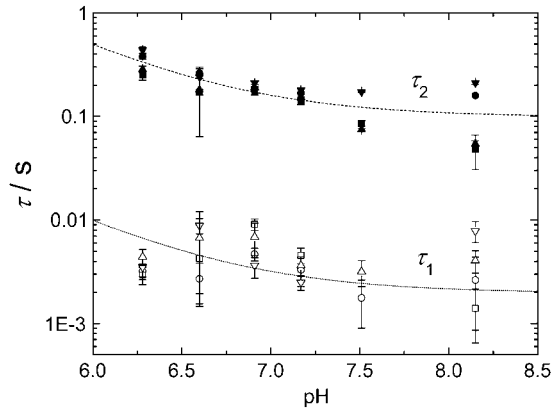

FIGURE 3 pH dependence of the Ca^{2+}-induced partial reactions. Both time constants τ_1 (*open symbols*) and τ_2 (*solid symbols*) were obtained from the fluorescence decrease (see Fig. 1) after the first (*square*), second (*circle*), third (*up-triangle*), and fourth (*down-triangle*) flash. The lines were drawn to guide the eye, the shape of the lower curve corresponds the upper curve, shifted by a factor of 50 to shorter times.

negligible Ca^{2+} concentrations (<3 nM), and in buffers with pH of 6.6, 7.2, and 7.8. To analyze the temperature dependence, the time constants were represented as an Arrhenius plot, as shown in Fig. 4. The data sets obtained from measurements in the same buffer could be fitted by a regression line. The slope in the semilogarithmic plot is proportional to the activation energy of the rate-limiting process. For the temperature dependence of both time constants, different activation energies were found. The fast process showed an activation energy of 31.6 kJ mol^{-1} at pH 7.8, 42.3 kJ mol^{-1} at pH 7.2, and 50.6 kJ mol^{-1} at pH 6.6. The activation energy of the fast process is higher at lower pH. The slow process was characterized by an activation

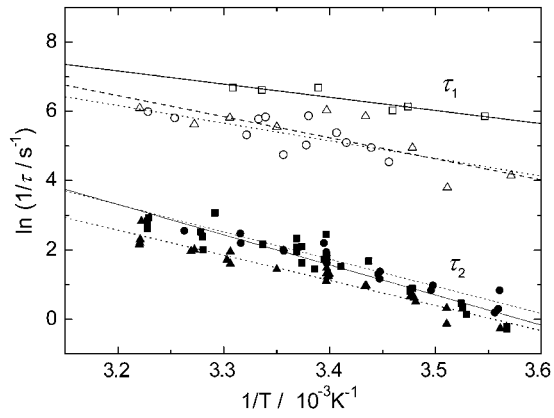

FIGURE 4 Temperature dependence of the relaxation-time constants. The experimentally determined time constants, τ_1 (*open symbols*) and τ_2 (*solid symbols*), are shown as Arrhenius plot. The flash-induced Ca^{2+} release was performed at different buffer pH (*square*, pH 7.8; *circle*, pH 7.2; and *up-triangle*, pH 6.6). The line drawn through the data are linear regression fits, and their slope, *m*, is proportional to the activation energy of the rate-limiting process, $E_A = -m \times R$ (*R* is the gas constant).

energy of 72.3 kJ mol^{-1} at pH 7.8, 65.2 kJ mol^{-1} at pH 7.2, and 60.3 kJ mol^{-1} at pH 6.6. The activation energy of the fast process is higher at higher pH.

DISCUSSION

The Ca^{2+} chelator DM-Nitrophen is able to generate a Ca^{2+}-concentration jump after an UV flash within microseconds (29). This method was applied to investigate Ca^{2+} binding to the SR Ca-ATPase for the first time in 1990 (30). In this study, the time dependence of the extravesicular Ca^{2+} concentration was monitored, and upon release from its cage, the Ca^{2+} concentration increased and, subsequently, due to the action of the Ca pump, a reduction of the free Ca^{2+} was observed. The time resolution was in the order of 20 ms. In the experiments presented here, Ca^{2+} uptake into the membrane domain of the Ca-ATPase was detected with a time resolution of typically 100 μs.

After the UV flash-triggered release of Ca^{2+} resulting in concentration jumps between 30 nM and 450 nM, two processes could be resolved by analysis of the 2BITC-fluorescence decrease with Eq. 1. The fast process is described by τ_1, which had values between 2 ms and 8 ms, and the slow process with 50 ms $< \tau_2 <$ 200 ms. We estimated the dependence of the two processes on pH, Ca^{2+} concentration and temperature.

Both time constants were not significantly dependent on the free Ca^{2+} concentration above the limiting 50 nM. The time constant of the faster process, τ_1, was averaged to 4.7 $\pm$ 0.5 ms at $T = 20°C$. A small increase of τ_1 could be observed in the range of pH $<$ 7.5 (Fig. 3). This tendency became more evident when the temperature dependence of τ_1 was investigated at different pH values, as shown in Fig. 4. The Arrhenius plot reveals a clear shift of the values of $1/\tau_1$ in buffer of pH 7.8 when compared to pH 7.2 and pH 6.6. And, what is more significant, the activation energy of the fast process, as determined from the temperature-dependence of $1/\tau_1$, was pH-dependent too—namely, 31.6 kJ mol^{-1} at pH 7.8, 42.3 kJ mol^{-1} at pH 7.2, and 50.6 kJ mol^{-1} at pH 6.6. The activation energy of the fast process was increased at higher concentrations of protons.

Similarly to the faster process, the time-constant of the slower process, τ_2, was also independent of the Ca^{2+} concentration and approximately a factor-of-50 larger than τ_1 (Fig. 2 *A*). It is, in the same way, pH-dependent as τ_1 (Fig. 2 *A*). When the pH was reduced from 8.15 to 6.28, τ_2 increases by a factor of 3.5. Significant differences were also found in the analysis of the temperature dependence. The Arrhenius plot showed a higher activation energy for the slower process than for the fast one at all buffer pH values. The activation energy for the slower process decreased with the proton concentration of the buffer and is 60.3 kJ mol^{-1} at pH 6.6, 65.2 kJ mol^{-1} at pH 7.2, and 72.3 kJ mol^{-1} at pH 7.8.

The reaction steps that follow the flash-induced Ca^{2+} release occur according to the Post-Albers scheme with the sequence $H_xE_1 \leftrightarrow E_1 \leftrightarrow Ca_yE_1$, with $0 \le x \le 3$ and $0 \le y \le 2$ (x is the number of protons bound to the ion pump in the E_1 conformation and depends on buffer pH; y is the number of Ca^{2+} bound after the concentration jump, when the protein reached equilibrium). The number of bound protons in E_1 state is discussed in literature to be two, three, or four (31–34). The binding of protons is characterized to be in competition with the binding of other ion species (35). We were able to simulate the binding of protons to the E_1 state with a linear binding scheme and, according to Peinelt and Apell (2), the distribution of the different states are at pH 8 ~30% E_1, 30% HE_1, 30% H_2E_1, and at pH 6 ~50% H_2E_1, 50% H_3E_1.

In contrast to the time constant τ_1, the respective fluorescence amplitude F_1 showed a binding affinity for Ca^{2+} in agreement with the published equilibrium dissociation constants for Ca^{2+}. This observation may be explained by the fact that the rate constant is controlled by the rate-limiting step of the relaxation process, which is not necessarily the Ca^{2+} migration into the binding site and binding inside the membrane domain of the protein, whereas the fluorescence decrease reports the amount of positive charge in the binding sites. The apparently Ca^{2+}-independent fluorescence amplitude of the slower process, F_2, has to be seen in the light of the high binding affinity of the second Ca^{2+} site. Therefore, it can be expected that the second Ca^{2+} is immediately bound when the site becomes available at the given Ca^{2+} concentrations (2). The maximum fluorescence decrease of -2% for the fast process and -2.7% for the slow process indicate that less (net) charge was imported during the faster first reaction step. This may be explained by the fact that due to a pK 8 of the binding sites in E_1 (2), part of the binding sites were occupied by a proton which is exchanged against a Ca^{2+}, thus reducing the net amount of charge imported.

The analyzed processes cannot be explained as simple binding of ions. First, ion binding would be a second-order reaction and, therefore, the rate constant has to be Ca^{2+}-concentration dependent. Second, ion binding is a diffusion-controlled process, which would occur in a time period below 1 ms. Third, simple binding of ions cannot account for the observed high activation energy. Ion binding in terms of a transfer from its hydrated form into a moiety mimicking a hydration shell has typically a low activation energy in the order of 5–10 kJ mol^{-1}.

Ca^{2+} binding to the E_1 conformation from the cytosol was shown to be a single-file process by Ca^{2+} exchange experiments performed with radioactive Ca^{2+} by Inesi and collaborators (1,17,22). The first ion binds and causes a conformation relaxation, a pre-occlusion of the first ion, and the high-affinity binding site for the second ion then becomes accessible (17,36). A similar conformational rearrangement may be postulated also for the enzyme after the release of the (last) proton and before binding of the first Ca^{2+}. Therefore, the linear ion-binding and release sequence of the Post-Albers cycle in the E_1 conformation is expanded by two additional steps whose kinetics are slow in

comparison to the electrogenic diffusion of the ions and their coordination in the sites:

$$HE_1^* \overset{fast}{\rightleftarrows} E_1^* \overset{slow}{\rightleftarrows} E_1 \overset{fast}{\rightleftarrows} CaE_1 \overset{slow}{\rightleftarrows} CaE^{**}_1 \overset{fast}{\rightleftarrows} Ca_2E^{**}_1.$$

In the Ca^{2+}-concentration jump experiments, upon Ca^{2+} release the equilibrium is shifted from left to right. The extent of the shift depends on buffer pH and the Ca^{2+} concentration before and after the release from the caged compound. Both experimentally determined time constants, τ_1 and τ_2, are interpreted as relaxation times of the reaction steps, $E_1^* \leftrightarrow E_1$ and $CaE_1 \leftrightarrow CaE_1^{**}$, respectively, and are functions of the forward and backward rate constants, $\tau = (k_{for} + k_{back})^{-1}$. The rate constants themselves could not be deduced with the experiments performed.

A comprehensive reaction model has to account for the fact that the kinetics is independent of the free Ca^{2+} concentration in the buffer and only weakly dependent on pH. Each of the two processes facilitates binding of one Ca^{2+}, and the faster process displaces, in addition, one proton from inside the membrane domain. Both processes should include conformational relaxations to account for the high activation energy.

With respect to the structure of the membrane domain of the SR Ca-ATPase, the membrane helix M6 and the loop L67 are promising candidates to suggest a molecular mechanism that explains the observed behavior. In the literature, pre-ion-binding of Ca^{2+} to the cytoplasmic loop L67 is already introduced. It is discussed as a transfer location for the ions into their binding sites inside the membrane domain (37,38). This loop is located between the sixth and seventh transmembrane helix and consists of a 20-amino-acid peptide beginning with Gly^{808} close to the entrance to the ion-binding sites. A synthetic peptide of identical sequence was shown to form Ca^{2+} complexes (39), and Ca-ATPase mutants with two or three of the aspartate residues in the L67 sequence replaced by alanine reveal a significantly lower Ca-ATPase activity than the wild-type (37). Lenoir and collaborators showed by fluorescence experiments with isothiocyanate-labeled protein a reduced Ca^{2+} affinity in Ca-ATPase mutants modified at Asp^{813}, Asp^{815}, and Asp^{818} (40). Loop L67 may act as a guidance device by transiently binding a Ca^{2+} to these three aspartate side chains and facilitating the entry mechanism of the ions (38), probably by a movement of the ion-loaded loop.

Although Lenoir and collaborators modified their proposal on the role of the L67 loop (40), such a L67-supported Ca^{2+}-entry mechanism would provide a suitable explanation for the experimental findings presented here. The two analyzed processes are assumed to be a movement of L67 as rate-limiting steps before binding of each Ca^{2+} inside the enzyme, and can be identified as the two conformational relaxations, whereby the time-constant τ_1 represents $E_1^* \rightarrow E_1$ and τ_2 represents $CaE_1 \rightarrow CaE_1^{**}$. Assuming that loading of the ion-binding sites is more effective when facilitated by a L67-loop movement, the first bound Ca^{2+} will reduce the mobility of L67 by coordination with Thr^{799} and Asp^{800} on the helix M6. On one hand such a fixation of M6 by the Ca^{2+} might be essential for the formation of the second Ca^{2+}-binding site, and on the other hand it may explain also the deceleration of the kinetics of the second partial reaction analyzed, $CaE_1 \leftrightarrow CaE_1^{**} \leftrightarrow Ca_2E_1^{**}$. This concept is supported by the significantly lower activation energies of 30–50 kJ mol^{-1} for the fast process compared to 60–72 kJ mol^{-1} for the slow process. Binding of the first Ca^{2+} inside the protein affects M6, and therefore, it can change the kinetical properties of the conformational relaxation of L67 loaded with the second Ca^{2+}. The activation energy of the L67 movement loaded with the second Ca^{2+} will be higher than the L67 movement with the first Ca^{2+} ion and a non-occupied binding site I. The comparable pH dependence of both time constants cannot be assigned to interactions of the protons with the high-affinity Ca^{2+} binding sites of the pump due to the fact that no significant competition with Ca^{2+} was observed. An alternative explanation could be the binding of a proton to an allosteric site from which it has to dissociate before the conformational relaxation may occur. A possible mechanistic explanation can also be related to loop L67, which contains three aspartate residues (Asp^{813}, Asp^{815}, and Asp^{818}) whose carboxylic side chains might be protonated. A buffer pH below 7 could result in a protonation of one (or more) aspartate residues and thereby slightly reduce the Ca^{2+} affinity. If only the Ca-loaded-L67 is able to perform a conformational rearrangement, the rate of 2BITC-detected Ca^{2+} binding to site I will be decreased at low pH. The slower Ca^{2+} binding at the L67 site leads to increased τ_1 and τ_2 at low pH as shown in Fig. 3.

CONCLUSION

Binding of two Ca^{2+} ions to the SR Ca-ATPase in the E_1 conformation is a multistep process that consists of two rate-limiting conformational relaxations with time constants τ_1 and τ_2, which precede the electrogenic binding of the first and the second Ca^{2+}. This result is in agreement with the observation of published binding studies with tracer Ca^{2+}, showing that the second binding site becomes available only after occupation of the first site. The data also support the proposal that each Ca^{2+} is bound transiently to the cytoplasmic loop L67, which provides an entry mechanism for Ca^{2+} by a spatial rearrangement to guide the ions into the access channel to the binding sites inside the membrane domain of the pump.

We thank Milena Roudna for excellent technical assistance. We also thank Dr. Andreas Beck and Dr. Stefan Alfred Gross for carefully reading the manuscript.

This work was financially supported by the Deutsche Forschungsgemeinschaft (Ap 45/4).

REFERENCES

1. Läuger, P. 1991. Electrogenic Ion Pumps. Sinauer, Sunderland, MA.
2. Peinelt, C., and H.-J. Apell. 2002. Kinetics of the Ca^{2+}, H^+, and Mg^{2+} interaction with the ion-binding sites of the SR-Ca-ATPase. *Biophys. J.* 82:170–181.
3. Peinelt, C., and H. J. Apell. 2004. Time-resolved charge movements in the sarcoplasmatic reticulum Ca-ATPase. *Biophys. J.* 86:815–824.
4. Apell, H. J. 2004. How do P-type ATPases transport ions? *Bioelectrochemistry.* 63:149–156.
5. Toyoshima, C., M. Nakasako, H. Nomura, and H. Ogawa. 2000. Crystal structure of the calcium pump of sarcoplasmatic reticulum at 2.6 Å resolution. *Nature.* 405:647–655.
6. Toyoshima, C., and H. Nomura. 2002. Structural changes in the calcium pump accompanying the dissociation of calcium. *Nature.* 418:605–611.
7. Toyoshima, C., H. Nomura, and Y. Sugita. 2003. Crystal structures of Ca^{2+}-ATPase in various physiological states. *Ann. N. Y. Acad. Sci.* 986:1–8.
8. Toyoshima, C., and T. Mizutani. 2004. Crystal structure of the calcium pump with a bound ATP analogue. *Nature.* 430:529–535.
9. Olesen, C., T. Sørensen, R. C. Nielsen, J. V. Moller, and P. Nissen. 2004. Dephosphorylation of the calcium pump coupled to counterion occlusion. *Science.* 306:2251–2255.
10. Sørensen, T., J. V. Moller, and P. Nissen. 2004. Phosphoryl transfer and calcium ion occlusion in the calcium pump. *Science.* 304:1672–1675.
11. Pedersen, M., M. Roudna, S. Beutner, M. Birmes, B. Reifers, H.-D. Martin, and H.-J. Apell. 2002. Detection of charge movements in ion pumps by a family of styryl dyes. *J. Membr. Biol.* 185:221–236.
12. Ellis-Davies, G. C., and J. H. Kaplan. 1994. Nitrophenyl-EGTA, a photolabile chelator that selectively binds Ca^{2+} with high affinity and releases it rapidly upon photolysis. *Proc. Natl. Acad. Sci. USA.* 91: 187–191.
13. Kaplan, J. H., and G. C. Ellis-Davies. 1988. Photolabile chelators for the rapid photorelease of divalent cations. *Proc. Natl. Acad. Sci. USA.* 85:6571–6575.
14. Chen, B., T. C. Squier, and D. J. Bigelow. 2004. Calcium activation of the Ca-ATPase enhances conformational heterogeneity between nucleotide binding and phosphorylation domains. *Biochemistry.* 43: 4366–4374.
15. Sørensen, T. L., Y. Dupont, B. Vilsen, and J. P. Andersen. 2000. Fast kinetic analysis of conformational changes in mutants of the Ca^{2+}-ATPase of sarcoplasmic reticulum. *J. Biol. Chem.* 275:5400–5408.
16. Dupont, Y. 1980. Occlusion of divalent cations in the phosphorylated calcium pump of sarcoplasmic reticulum. *Eur. J. Biochem.* 109:231–238.
17. Inesi, G. 1987. Sequential mechanism of calcium binding and translocation in sarcoplasmic reticulum adenosine triphosphatase. *J. Biol. Chem.* 262:16338–16342.
18. Khananshvili, D., and W. P. Jencks. 1988. Two-step internalization of Ca^{2+} from a single E-P·Ca_2 species by the Ca^{2+}-ATPase. *Biochemistry.* 27:2943–2952.
19. Petithory, J. R., and W. P. Jencks. 1988. Sequential dissociation of Ca^{2+} from the calcium adenosinetriphosphatase of sarcoplasmic reticulum and the calcium requirement for its phosphorylation by ATP. *Biochemistry.* 27:5553–5564.
20. Tanford, C., J. A. Reynolds, and E. A. Johnson. 1987. Sarcoplasmatic reticulum calcium pump: A model for Ca^{2+} binding and Ca^{2+} coupled phosphorylation. *Proc. Natl. Acad. Sci. USA.* 84:7094–7098.
21. Inesi, G., Z. Zhang, and D. Lewis. 2002. Cooperative setting for long-range linkage of Ca^{2+} binding and ATP synthesis in the Ca^{2+} ATPase. *Biophys. J.* 83:2327–2332.
22. Inesi, G., C. Sumbilla, and M. E. Kirtley. 1990. Relationships of molecular structure and function in Ca^{2+}-transport ATPase. *Physiol. Rev.* 70:749–760.
23. Toyoshima, C., and G. Inesi. 2004. Structural basis of ion pumping by Ca^{2+}-ATPase of the sarcoplasmic reticulum. *Annu. Rev. Biochem.* 73: 269–292.
24. Doyle, D. A., C. J. Morais, R. A. Pfuetzner, A. Kuo, J. M. Gulbis, S. L. Cohen, B. T. Chait, and R. MacKinnon. 1998. The structure of the potassium channel: molecular basis of K^+ conduction and selectivity. *Science.* 280:69–77.
25. Vilsen, B., and J. P. Andersen. 1998. Mutation to the glutamate in the fourth membrane segment of Na^+,K^+-ATPase and Ca^{2+}-ATPase affects cation binding from both sides of the membrane and destabilizes the occluded enzyme forms. *Biochemistry.* 37:10961–10971.
26. Orlowski, S., and P. Champeil. 1991. The two calcium ions initially bound to nonphosphorylated sarcoplasmic reticulum Ca^{2+}-ATPase can no longer be kinetically distinguished when they dissociate from phosphorylated ATPase toward the lumen. *Biochemistry.* 30:11331–11342.
27. Pedersen, A., and P. L. Jorgensen. 1992. Expression of Na,K-ATPase in *Saccharomyces cerevisiae*. *Ann. N. Y. Acad. Sci.* 671:452–454.
28. Heilmann, C., D. Brdiczka, E. Nickel, and D. Pette. 1977. ATPase activities, Ca^{2+} transport and phosphoprotein formation in sarcoplasmic reticulum subfractions of fast and slow rabbit muscles. *Eur. J. Biochem.* 81:211–222.
29. Tsien, R. Y., and R. S. Zucker. 1986. Control of cytoplasmic calcium with photolabile tetracarboxylate 2-nitrobenzhydrol chelators. *Biophys. J.* 50:843–853.
30. DeLong, L. J., C. M. Phillips, J. H. Kaplan, A. Scarpa, and J. K. Blasie. 1990. A new method for monitoring the kinetics of calcium binding to the sarcoplasmic reticulum Ca^{2+}-ATPase employing the flash-photolysis of caged-calcium. *J. Biochem. Biophys. Methods.* 21:333–339.
31. Yu, X., S. Carroll, J. L. Rigaud, and G. Inesi. 1993. H^+ countertransport and electrogenicity of the sarcoplasmic reticulum Ca^{2+} pump in reconstituted proteoliposomes. *Biophys. J.* 64:1232–1242.
32. Yu, X., and G. Inesi. 1993. Effects of anions on the Ca^{2+}, H^+ and electrical gradients formed by the sarcoplasmic reticulum ATPase in reconstituted proteoliposomes. *FEBS Lett.* 328:301–304.
33. Yu, X., L. Hao, and G. Inesi. 1994. A pK change of acidic residues contributes to cation countertransport in the Ca-ATPase of sarcoplasmic reticulum. Role of H^+ in Ca^{2+}-ATPase countertransport. *J. Biol. Chem.* 269:16656–16661.
34. Levy, D., M. Seigneuret, A. Bluzat, and J. L. Rigaud. 1990. Evidence for proton countertransport by the sarcoplasmic reticulum Ca^{2+}-ATPase during calcium transport in reconstituted proteoliposomes with low ionic permeability. *J. Biol. Chem.* 265:19524–19534.
35. Forge, V., E. Mintz, and F. Guillain. 1993. Ca^{2+} binding to sarcoplasmic reticulum ATPase revisited. I. Mechanism of affinity and cooperativity modulation by H^+ and Mg^{2+}. *J. Biol. Chem.* 268:10953–10960.
36. Inesi, G., and M. E. Kirtley. 1990. Coupling of catalytic and channel function in the Ca^{2+} transport ATPase. *J. Membr. Biol.* 116:1–8.
37. Falson, P., T. Menguy, F. Corre, L. Bouneau, A. G. de Gracia, S. Soulie, F. Centeno, J. V. Moller, P. Champeil, and M. le Maire. 1997. The cytoplasmic loop between putative transmembrane segments 6 and 7 in sarcoplasmic reticulum Ca^{2+}-ATPase binds Ca^{2+} and is functionally important. *J. Biol. Chem.* 272:17258–17262.
38. Menguy, T., F. Corre, B. Juul, L. Bouneau, D. Lafitte, P. J. Derrick, P. S. Sharma, P. Falson, B. A. Levine, J. V. Moller, and M. le Maire. 2002. Involvement of the cytoplasmic loop L6–7 in the entry mechanism for transport of Ca^{2+} through the sarcoplasmic reticulum Ca^{2+}-ATPase. *J. Biol. Chem.* 277:13016–13028.
39. Menguy, T., F. Corre, L. Bouneau, S. Deschamps, J. V. Møller, P. Champeil, M. le Maire, and P. Falson. 1998. The cytoplasmic loop located between transmembrane segments 6 and 7 controls activation by Ca^{2+} of sarcoplasmic reticulum Ca^{2+}-ATPase. *J. Biol. Chem.* 273:20134–20143.
40. Lenoir, G., M. Picard, J. V. Moller, M. le Maire, P. Champeil, and P. Falson. 2004. Involvement of the L6–7 loop in SERCA1a Ca^{2+}-ATPase activation by Ca^{2+} (or Sr^{2+}) and ATP. *J. Biol. Chem.* 279:32125–32133.